J. Marine Sci. Appl. (2012) 11: 276-285
DOI: 10.1007/s11804-012-1133-2

Oblique Water Wave Scattering by Bottom Undulation in a Two-layer Fluid Flowing Through a Channel

Smrutiranjan Mohapatra[1*] and Swaroop Nandan Bora[2]

1. Department of Mathematics, Institute of Chemical Technology, Mumbai 400019, India
2. Department of Mathematics, Indian Institute of Technology Guwahati, Guwahati 781039, India

Abstract: The problem of oblique wave (internal wave) propagation over a small deformation in a channel flow consisting of two layers was considered. The upper fluid was assumed to be bounded above by a rigid lid, which is an approximation for the free surface, and the lower one was bounded below by an impermeable bottom surface having a small deformation; the channel was unbounded in the horizontal directions. Assuming irrotational motion, the perturbation technique was employed to calculate the first-order corrections of the velocity potential in the two fluids by using Green's integral theorem suitably with the introduction of appropriate Green's functions. Those functions help in calculating the reflection and transmission coefficients in terms of integrals involving the shape function $c(x)$ representing the bottom deformation. Three-dimensional linear water wave theory was utilized for formulating the relevant boundary value problem. Two special examples of bottom deformation were considered to validate the results. Consideration of a patch of sinusoidal ripples (having the same wave number) shows that the reflection coefficient is an oscillatory function of the ratio of twice the x-component of the wave number to the ripple wave number. When this ratio approaches one, the theory predicts a resonant interaction between the bed and the interface, and the reflection coefficient becomes a multiple of the number of ripples. High reflection of incident wave energy occurs if this number is large. Similar results were observed for a patch of sinusoidal ripples having different wave numbers. It was also observed that for small angles of incidence, the reflected energy is greater compared to other angles of incidence up to $\pi / 4$. These theoretical observations are supported by graphical results.

Keywords: two-layer fluid; oblique waves; wave scattering; reflection coefficient; transmission coefficient; linear water wave theory; perturbation technique; Bottom Undulation
Article ID: 1671-9433(2012)03-0276-10

1 Introduction

The problems of channel flow consisting of a two-layer fluid over an obstacle or a geometrical disturbance at the bottom of the channel hold importance for their possible applications in the areas of coastal and marine engineering. The problem of reflection of oblique waves by patches of bottom deformation has received a reasonable amount of attention as its mechanism is important in the development of bottom-parallel bars or pipes. Two-layer fluid problems in a finite depth are not very difficult to formulate mathematically within the framework of linearised theory, yet the available literature on this subject is rather sparse.

The linearised theory of small amplitude waves in two superposed inviscid fluids, separated by a common interface with the total fluid region bounded above and below by rigid horizontal walls, is given in the treatise by Lamb (1932). In such a two-layer fluid region, only one wave mode can exist for a given frequency; time-harmonic gravity waves can propagate in either direction at the interface. A train of progressive interface waves traveling over the bottom surface of a channel, without any obstacle, experiences no reflection when the channel is of uniform finite depth. If the bed of the channel has a deformation, the wave train is partially reflected by it, and is partially transmitted over it. However, there exists a class of mostly naturally occurring bottom standing obstacles such as sand ripples. These ripples can be assumed to be small in some sense, for which some sort of perturbation technique can be employed for obtaining the first order corrections to the reflection and transmission coefficients. Linton and McIver (1995) developed a general theory for two-dimensional wave scattering by horizontal cylinders in an infinitely deep two-layer fluid, and calculated the amount of energy that was converted from one wave number to the other for the case of circular cylinders in either of the upper or the lower layer by employing the multipole expansion method. The motivation for this work arose due to the plan to build an underwater pipe bridge across one of the Norwegian fjords, which consist of a layer of fresh water on top of a deep layer of salt water. Linton and Cadby (2002) extended the work of Linton and McIver (1995) to oblique scattering, and later Chamberlain and Porter (2005) examined the scattering of waves in a two-layer fluid of varying mean depth in a three-dimensional context by using linear theory. A variational technique was used to construct a particular type

Received date: 2011-09-03.
***Corresponding author Email:** sr.mohapatra@ictmumbai.edu.in

of approximation which had the effect of removing the vertical coordinate and reducing the problem to two coupled partial differential equations in two independent variables.

Kassem (1986) discussed the different types of basic singularities that arose in one of the layers and obtained the velocity potentials describing the line and point multipoles when each layer was of finite constant depth. With the free surface approximated by a rigid lid, Sturova (1994) studied the radiation of waves by an oscillating cylinder moving uniformly in a direction perpendicular to its axis. Later on, Sturova (1999) also considered the radiation and scattering problem for a cylinder in both two-layer and three-layer fluids bounded above and below by rigid horizontal walls. Using the method of multipoles, Sturova was able to calculate the hydrodynamic characteristics of the cylinder. Bhatta and Debnath (2006) analyzed a transient two-layer fluid flow over a viscoelastic ocean bed by using the Laplace transform and the Fourier transform. Davies (1982) solved the refection of normally incident surface waves by a patch of sinusoidal deformations on the sea-bed in a finite region by using the Fourier transform technique. Miles (1981) obtained approximately the reflection and transmission coefficients up to the first order in terms of integrals involving a small cylindrical deformation of the bottom by using small perturbation theory when the wave train, propagating in a single-layer fluid, was obliquely incident.

Mandal and Basu (1993, 1996) employed perturbation analysis while solving the problem of water wave diffraction of interface waves by bottom deformation of two laterally unbounded superposed fluids. They considered the problem for the normal as well as oblique interface waves when the upper layer was of infinite depth and then derived the reflection and transmission coefficients approximately up to the first order in terms of integrals involving the shape function representing the bottom elevation. Maity and Mandal (2006) employed Green's function technique to study the reflection of oblique surface waves over small deformations in a two-layer fluid which had a free surface. Mohapatra and Bora (2009a) considered the water wave interaction with a sphere in a two-layer fluid flowing in a channel of finite depth. Using a method of multiple expansions, they derived the added-mass, damping coefficients, and exciting forces due to heave and sway motions.

Mohapatra and Bora (2009b, 2011) considered the scattering of normal internal wave propagation over a small deformation on the bottom of an ocean for a two-layer fluid. A perturbation technique was employed to reduce the original boundary value problem to a coupled boundary value problem up to the first order, and the velocity potential, reflection coefficient, and transmission coefficient up to the first order were obtained by using Green's function technique and the Fourier transform. The present work is the extension of the previous work (Mohapatra and Bora, 2009b) to oblique scattering. Two laterally unbounded superposed fluids are considered with the fluid domain in the form of a long cylinder extending in the lateral direction, in which upper fluid is bounded above by a rigid lid and the lower one bounded by a bottom surface which has small deformation. The free surface, i.e., the surface above the upper layer, has been replaced and approximated by a rigid lid rendering the flow to a channel flow. Applying perturbation technique with a small parameter ε directly to the governing boundary value problem (BVP), the original problem is reduced to a simpler BVP for the first order correction of the potentials. The solution of this BVP is then obtained by an appropriate application of Green's integral theorem to the potential functions describing the BVP. The reflection and transmission coefficients are evaluated approximately up to the first order of ε in terms of integrals involving the shape function when a train of progressive waves propagating from negative infinity is obliquely incident on the channel bed having small deformations. Two different special forms of bottom deformation are presented, namely, a patch of sinusoidal ripples having the same wave number and a patch of sinusoidal ripples having two different wave numbers for two consecutive stretches.

2 Mathematical formulation of the problem

The irrotational motion of a two-layer inviscid incompressible fluid flow under a rigid infinite lid through a channel which is bounded by a bottom surface with small cylindrical deformation is considered. A right-handed Cartesian coordinate system is used in which the $xz-$plane coincides with the undisturbed surface between the two fluids. The y-axis points vertically downwards with $y=0$ as the interface and $y=-h'$ as the position of the rigid lid. Here, the bottom of the lower layer with small deformation is described by $y=h+\varepsilon c(x)$, where $c(x)$ is a smooth function with compact support, h the uniform finite depth of the lower layer fluid far to either side of the deformation of the bottom so that $c(x)\to 0$ as $|x|\to\infty$ and the non-dimensional number $\varepsilon(<<1)$ a measure of smallness of the deformation (Fig. 1). The rigid infinite lid at $y=-h'$ can be considered to be an approximation to the free surface. Under the assumptions of linear water wave theory, the time harmonic velocity potential in the lower fluid of density ρ_1 can be described by $\mathrm{Re}\left[\phi(x,y)\mathrm{e}^{\mathrm{i}\upsilon z}\mathrm{e}^{-\mathrm{i}\sigma t}\right]$ and that in the upper layer fluid of density $\rho_2<\rho_1$ by $\mathrm{Re}\left[\psi(x,y)\mathrm{e}^{\mathrm{i}\upsilon z}\mathrm{e}^{-\mathrm{i}\sigma t}\right]$, where the potentials ϕ and ψ, respectively, must satisfy the modified Helmholtz equation:

$$\left(\nabla_{x,y}^2-\upsilon^2\right)\phi=0 \quad \text{in lower fluid} \tag{1}$$

$$\left(\nabla_{x,y}^2 - \upsilon^2\right)\psi = 0 \quad \text{in upper fluid} \tag{2}$$

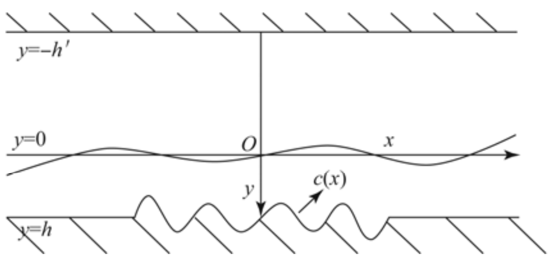

Fig. 1 Domain definition sketch

The linearized boundary conditions at the bottom of the channel, on the interface and at the lid are

$$\frac{\partial \phi}{\partial n} = 0 \quad \text{on} \quad y = h + \varepsilon c(x) \tag{3}$$

$$\frac{\partial \phi}{\partial y} = \frac{\partial \psi}{\partial y} \quad \text{on} \quad y = 0 \tag{4}$$

$$K\phi + \frac{\partial \phi}{\partial y} = \rho\left(K\psi + \frac{\partial \psi}{\partial y}\right) \quad \text{on} \quad y = 0 \tag{5}$$

$$\frac{\partial \psi}{\partial y} = 0 \quad \text{on} \quad y = -h' \tag{6}$$

With $K = \sigma^2/g$, σ denoting the angular frequency of incoming waves, g the acceleration due to gravity, $\rho = \rho_2/\rho_1 (<1)$ and $\partial/\partial n$ the derivative normal to the bottom at a point (x, y). The time dependence of $\mathrm{e}^{-\mathrm{i}\sigma t}$ has been suppressed. The boundary conditions (4) and (5), respectively, represent the continuity of the normal velocity and the pressure at the interface.

Within this framework in a two-layer fluid, a train of progressive interface-waves takes the form (up to an arbitrary multiplicative constant) $\phi_0(x,y)\mathrm{e}^{\mathrm{i}\upsilon z}$ and $\psi_0(x,y)\mathrm{e}^{\mathrm{i}\upsilon z}$ in the lower and upper layer fluids, respectively, where

$$\phi_0(x,y) = \frac{\cosh u(h-y)}{\sinh uh}\mathrm{e}^{\mathrm{i}\mu x} \tag{7}$$

$$\psi_0(x,y) = -\frac{\cosh u(h'+y)}{\sinh uh'}\mathrm{e}^{\mathrm{i}\mu x} \tag{8}$$

which is obliquely incident upon the bottom deformation from negative infinity. Here $\mu = u\cos\theta$, $\upsilon = u\sin\theta$ with θ as the angle of oblique incidence of progressive interface waves and u satisfying the dispersion relation $\Delta(u) = 0$, where

$$\Delta(u) = \frac{K\left(\cosh uh \sinh uh' + \rho \sinh uh \cosh uh'\right)}{1-\rho} - u\sinh uh \sinh uh' \tag{9}$$

In the above equation, there is a positive real root k, which indicates the propagating modes of the fluid at the interface and a countable infinity of purely imaginary roots iu_n, $n = 1, 2, \ldots$ that relate to a set of evanescent modes, where u_n are real and positive satisfying

$$\frac{K\left(\cos\kappa h \sin\kappa h' + \rho\sin\kappa h\cos\kappa h'\right)}{1-\rho} + \kappa\sin\kappa h\sin\kappa h' = 0$$

The intensity of the evanescent mode of waves decays exponentially with distance from the interface at which they are formed. Due to this evanescent mode of waves appearing in the fluid region, a part of the incident interfacial wave becomes trapped and leads to a standing wave pattern over the bottom irregularities, when the incident wave is scattered by the bottom undulation. This phenomenon is called "Anderson localization". More precisely, this implies that a periodic plane wave of finite wavelength coming on to the part of the channel with a random bottom will eventually be totally reflected, i.e., the amplitude of the disturbance created by the wave will die off exponentially with distance, with a typical length which is called the localization length. But these waves do not affect the asymptotic behavior of the resultant reflected and transmitted waves. In that sense, any sort of localization is not considered while formulating and solving the present problem.

The negatives of all roots of are also roots, being wave numbers of the waves travelling in the opposite direction. As Eq.(9) has one nonzero positive simple zero at $u = k$, for example, on the real axis of u, so only one nonzero wave number k can exist and the wave can propagate in either direction. Note that if $k = 0$, then there is no wave in the respective regions.

The wave train, given by $\phi_0(x,y)\mathrm{e}^{\mathrm{i}\upsilon z}$ and $\psi_0(x,y)\mathrm{e}^{\mathrm{i}\upsilon z}$, is partially reflected by and partially transmitted over the bottom deformation so that the far-field behaviors of ϕ and ψ are given by

$$\phi(x,y) \sim \begin{cases} T\phi_0(x,y) & x \to \infty \\ \phi_0(x,y) + R\phi_0(-x,y) & x \to -\infty \end{cases} \tag{10}$$

$$\psi(x,y) \sim \begin{cases} T\psi_0(x,y) & x \to \infty \\ \psi_0(x,y) + R\psi_0(-x,y) & x \to -\infty \end{cases} \tag{11}$$

where R and T, respectively, represent the reflection and transmission coefficients due to an oblique incident wave, defined to be the ratio of amplitudes of the reflected and transmitted waves, respectively, to that of the incident wave and are to be determined.

Assuming, for small bottom deformation, ε to be very small and neglecting the second order terms, the boundary condition $\partial\phi/\partial n = 0$ on the bottom surface $y = h + \varepsilon c(x)$ can be converted to the following appropriate form:

$$\frac{\partial \phi}{\partial y} - \varepsilon\frac{\partial}{\partial x}\left[c(x)\frac{\partial \phi}{\partial x}\right] + O\left(\varepsilon^2\right) = 0 \quad \text{on} \quad y = h \tag{12}$$

The lower layer $y = h + \varepsilon c(x), -\infty < x < \infty$, decreases to the uniform strip $0 < y < h, -\infty < x < \infty$ in the following mathematical analysis where a perturbation technique is used.

3 Method of solution

3.1 Perturbation technique

Suppose that a train of progressive interface waves is obliquely incident at an angle $\theta, 0 \le \theta < \pi/2$ on the bottom deformation. If there is no bottom deformation, then the incident wave train will propagate without any hindrance and there will be only transmission. This, along with the appropriate form of the boundary condition (12), suggests that ϕ, ψ, R, and T can be expressed in terms of the small parameter ε as

$$\left.\begin{aligned} \phi &= \phi_0 + \varepsilon\phi_1 + O(\varepsilon^2) \\ \psi &= \psi_0 + \varepsilon\psi_1 + O(\varepsilon^2) \\ T &= 1 + \varepsilon T_1 + O(\varepsilon^2) \\ R &= \varepsilon R_1 + O(\varepsilon^2) \end{aligned}\right\} \tag{13}$$

where ϕ_0, ψ_0 are given by Eqs.(7) and (8), respectively.

It must be noted that such a perturbation expansion ceases to be valid at Bragg resonance when the reflection coefficient becomes much larger than the undulation parameter ε, as pointed out by Mei (1985). Also, this theory is valid only for infinitesimal reflection and away from resonance. For large reflection, the perturbation series, as defined in (13), needs to be refined so that it can deal with the resonant case, which is reported in Mei (1985). Because of the fact that the obstacles in the form of undulations are small, the work here does not concern large reflection and hence will not take into account resonance while deriving the results. Using Eq.(13) in Eqs.(1), (2), (12), (4), (5), (6), (10), (11) and equating the first order terms of ε in both sides of the equations, it is found that the first order potentials ϕ_1 and ψ_1 satisfy a coupled boundary value problem described by

$$\left(\nabla^2_{x,y} - \upsilon^2\right)\phi_1 = 0 \quad \text{in} \quad 0 \le y \le h \tag{14}$$

$$\left(\nabla^2_{x,y} - \upsilon^2\right)\psi_1 = 0 \quad \text{in} \quad -h' \le y \le 0 \tag{15}$$

$$\frac{\partial \phi_1}{\partial y} = \frac{1}{\sinh kh}\left\{ \mathrm{i}\mu \frac{\mathrm{d}}{\mathrm{d}x}\left[c(x)\mathrm{e}^{\mathrm{i}\mu x}\right] - \upsilon^2 c(x)\mathrm{e}^{\mathrm{i}\mu x} \right\} \equiv p(x) \tag{16}$$
(say) on $y=h$

$$\frac{\partial \phi_1}{\partial y} = \frac{\partial \psi_1}{\partial y} \quad \text{on} \quad y = 0 \tag{17}$$

$$K\phi_1 + \frac{\partial \phi_1}{\partial y} = \rho\left(K\psi_1 + \frac{\partial \psi_1}{\partial y}\right) \quad \text{on} \quad y = 0 \tag{18}$$

$$\frac{\partial \psi_1}{\partial y} = 0 \quad \text{on} \quad y = -h' \tag{19}$$

$$\phi_1(x,y) \sim \begin{cases} T_1\phi_0(x,y), & x \to \infty \\ R_1\phi_0(-x,y), & x \to -\infty \end{cases} \tag{20}$$

$$\psi_1(x,y) \sim \begin{cases} T_1\psi_0(x,y), & x \to \infty \\ R_1\psi_0(-x,y), & x \to -\infty \end{cases} \tag{21}$$

To solve the above coupled boundary value problem described by Eqs.(14)–(19), two-dimensional source potentials (in terms of Green's function) are needed for the modified Helmholtz equation due to a source submerged in either of the two-layer fluids where each layer is of finite depth. When the source is submerged in the lower fluid at (ξ,η), where $0 < \eta < h$, then $G_1(x,y;\xi,\eta)$ and $G_2(x,y;\xi,\eta)$ are considered to be the source potentials in terms of Green's function for the lower and the upper layers, respectively. Similarly when the source is submerged in the upper layer at (ξ,η), where $-h' < \eta < 0$, then $G_3(x,y;\xi,\eta)$ and $G_4(x,y;\xi,\eta)$ are considered to be the source potentials in terms of Green's function for the lower and the upper layers, respectively.

3.2 Introduction of Green's functions

Green's function method is introduced for solving the above boundary value problem. Two-dimensional source potentials are obtained for the Helmholtz equation due to a line source submerged in either of the two finite layers of the fluid. Suppose the source is submerged in the lower layer fluid. Then the source potentials in terms of Green's functions $G_1(x,y;\xi,\eta)$ and $G_2(x,y;\xi,\eta)$ satisfy the following boundary value problem:

$$\left(\nabla^2_{x,y} - \upsilon^2\right)G_1 = 0 \quad \text{in} \quad 0 < y < h, \quad \text{except at} \quad (\xi,\eta) \tag{22}$$

$$\left(\nabla^2_{x,y} - \upsilon^2\right)G_2 = 0 \quad \text{in} \quad -h' < y < 0 \tag{23}$$

$$\frac{\partial G_1}{\partial y} = 0 \quad \text{on} \quad y = h \tag{24}$$

$$\frac{\partial G_1}{\partial y} = \frac{\partial G_2}{\partial y} \quad \text{on} \quad y = 0 \tag{25}$$

$$KG_1 + \frac{\partial G_1}{\partial y} = \rho\left(KG_2 + \frac{\partial G_2}{\partial y}\right) \quad \text{on } y = 0 \tag{26}$$

$$\frac{\partial G_2}{\partial y} = 0 \quad \text{on} \quad y = -h' \tag{27}$$

$$G_1 \sim K_0(\upsilon r) \quad \text{as} \quad r = \left[(x-\xi)^2 + (y-\eta)^2\right]^{1/2} \to 0 \tag{28}$$

where $K_0(\upsilon r)$ denotes the modified Bessel function of the second kind. Also G_1 and G_2 represent outgoing waves as $|x-\xi| \to \infty$. Solutions to the above boundary value problem are found in the following form:

$$G_1(x,y;\xi,\eta)=K_0(\upsilon r)-\frac{1-\rho}{1+\rho}K_0(\upsilon r_1)+ \frac{1}{\mu}\int_{\upsilon}^{\infty}\left[A(u)\cosh u(h-y)+B(u)\sinh uy\right]\cos\mu(x-\xi)\mathrm{d}u \tag{29}$$

$$G_2(x,y;\xi,\eta)=\frac{2}{1+\rho}K_0(\upsilon r)+ \frac{1}{\mu}\int_{\upsilon}^{\infty}\left[A_1(u)\cosh u(h'+y)+B_1(u)\sinh uy\right]\cos\mu(x-\xi)\mathrm{d}u \tag{30}$$

where $r_1=\left\{(x-\xi)^2+(y+\eta)^2\right\}^{1/2}$.

In order that the boundary conditions (22)–(28) are satisfied and for $|x-\xi|\to\infty$, the solutions $G_1(x,y;\xi,\eta)$ and $G_2(x,y;\xi,\eta)$, as $|x-\xi|\to\infty$, are given by

$$G_1(x,y;\xi,\eta)=-2\pi\mathrm{i}K\times \left[\frac{\sinh kh'\cosh k(h-\eta)\cosh k(h-y)}{(1-\rho)\Delta'(k)\mu\sinh kh}\right]\mathrm{e}^{\mathrm{i}\mu|x-\xi|} \tag{31}$$

$$G_2(x,y;\xi,\eta)=2\pi\mathrm{i}K\times \left[\frac{\cosh k(h-\eta)\cosh k(h'+y)}{(1-\rho)\Delta'(k)\mu}\right]\mathrm{e}^{\mathrm{i}\mu|x-\xi|} \tag{32}$$

where k is the real positive root of the equation $\Delta(u)=0$ and $\Delta'(k)$ denotes the derivative of $\Delta(u)$ at $u=k$.

Similarly, when the source term (ξ,η), where $\eta<0$, is submerged in the upper layer fluid, then the source potentials $G_3(x,y;\xi,\eta)$ and $G_4(x,y;\xi,\eta)$ satisfy the same boundary value problem (22)–(27), with G_1 replaced by G_3 and G_2 by G_4, and in addition, G_4 satisfies $G_4\sim K_0(\upsilon r_1)$ as $r_1=\left[(x-\xi)^2+(y+\eta)^2\right]^{1/2}\to 0$ and G_3,G_4 also represent outgoing waves as $|x-\xi|\to\infty$. Here also, solutions of G_3 and G_4 satisfying the boundary value problem given by Eqs.(22)–(27) are found in the following form:

$$G_3(x,y;\xi,\eta)=\frac{2\rho}{1+\rho}K_0(\upsilon r_1)+ \frac{1}{\mu}\int_{\upsilon}^{\infty}\left[C(u)\cosh u(h-y)+D(u)\sinh uy\right]\cos\mu(x-\xi)\mathrm{d}u \tag{33}$$

$$G_4(x,y;\xi,\eta)=K_0(\upsilon r_1)+\frac{1-\rho}{1+\rho}K_0(\upsilon r)+ \frac{1}{\mu}\int_{\upsilon}^{\infty}\left[C_1(u)\cosh u(h'+y)+D_1(u)\sinh uy\right]\cos\mu(x-\xi)\mathrm{d}u \tag{34}$$

In order to satisfy the respective boundary conditions and for $|x-\xi|\to\infty$, the source potentials in terms of Green's function $G_3(x,y;\xi,\eta)$ and $G_4(x,y;\xi,\eta)$ in this case, as $|x-\xi|\to\infty$, are obtained as

$$G_3(x,y;\xi,\eta)=2\pi\mathrm{i}\rho K\times \left[\frac{\cosh k(h'-\eta)\cosh k(h-y)}{(1-\rho)\Delta'(k)\mu}\right]\mathrm{e}^{\mathrm{i}\mu|x-\xi|} \tag{35}$$

$$G_4(x,y;\xi,\eta)=-2\pi\mathrm{i}\rho K\times \left[\frac{\sinh kh\cosh k(h'-\eta)\cosh k(h'+y)}{(1-\rho)\Delta'(k)\mu\sinh kh'}\right]\mathrm{e}^{\mathrm{i}\mu|x-\xi|} \tag{36}$$

If the angle of incidence is zero, the representation of the Green's functions when $|x-\xi|\to\infty$, given by (31), (32), (35), and (36), coincide with the corresponding source potentials obtained earlier in Mohapatra and Bora (2009b).

To calculate $\phi_1(\xi,\eta)$, where $(\xi,\eta),\ 0<\eta<h$, is submerged in the lower layer fluid, first Green's integral theorem is applied to $\phi_1(x,y)$ and $G_1(x,y;\xi,\eta)$ in the form

$$\int_C\left(\phi_1\frac{\partial G_1}{\partial n}-G_1\frac{\partial\phi_1}{\partial n}\right)\mathrm{d}s=0 \tag{37}$$

where C is a closed contour in the xy-plane consisting of the lines $y=0(-X\le x\le X)$, $y=h(-X\le x\le X)$, $x=\pm X\,(0\le y\le h)$, and a small circle of radius δ with a center at (ξ,η) and ultimately letting $X\to\infty$, $\delta\to 0$. Then there will be no contribution to the integral from the line $x=\pm X$, as ϕ_1, $G_1\to 0$ when $X\to\pm\infty$. Thus the resultant form of the integral Eq.(37) will be

$$-2\pi\phi_1(\xi,\eta)+\int_{-\infty}^{\infty}p(x)G_1(x,h;\xi,\eta)\mathrm{d}x+ \int_{-\infty}^{\infty}\left(\phi_1\frac{\partial G_1}{\partial y}-G_1\frac{\partial\phi_1}{\partial y}\right)_{y=0}\mathrm{d}x=0 \tag{38}$$

Again Green's integral theorem is applied to $\psi_1(x,y)$ and $G_2(x,y;\xi,\eta)$ in the form

$$\int_{C'}\left(\psi_1\frac{\partial G_2}{\partial n}-G_2\frac{\partial\psi_1}{\partial n}\right)\mathrm{d}s=0 \tag{39}$$

where C' is a closed counter consisting of the lines $y=-h'(-X\le x\le X)$, $y=0(-X\le x\le X)$, $x=\pm X\,(-h'\le y\le 0)$ and ultimately letting $X\to\infty$. Here, it is noted that $G_2(x,y;\xi,\eta)$ has no singularity in the upper region. Again there will be no contribution to the integral from the line $y=-h'$ due to the same boundary condition satisfied by ψ_1 and G_2 there. Thus the resultant integral Eq.(39) will be

$$\int_{-\infty}^{\infty}\left(\psi_1\frac{\partial G_2}{\partial y}-G_2\frac{\partial\psi_1}{\partial y}\right)_{y=0}\mathrm{d}x=0 \tag{40}$$

Now solving Eqs.(39) and (40) with the help of interface conditions at $y=0$, the result is

$$\phi_1(\xi,\eta) = \frac{1}{2\pi}\int_{-\infty}^{\infty} G_1(x,h;\xi,\eta)p(x)\mathrm{d}x\,,\quad 0<\eta<h \tag{41}$$

which solves the boundary value problem for $\phi_1(x,y)$.

Similarly, to calculate $\psi_1(\xi,\eta)$, where the source term $(\xi,\eta),\quad -h'<\eta<0$, is submerged in the upper layer fluid, the same procedure will be applied as followed previously for the case of the lower layer fluid. The final expression for $\psi_1(\xi,\eta)$ is found as

$$\psi_1(\xi,\eta) = \frac{1}{2\pi\rho}\int_{-\infty}^{\infty} G_3(x,h;\xi,\eta)p(x)\mathrm{d}x \tag{42}$$

which solves the boundary value problem for $\psi_1(x,y)$.

4 Reflection and transmission coefficients

The first-order reflection and transmission coefficients R_1 and T_1, respectively, due to the oblique interfacial wave propagation, are now obtained by letting $\xi\to-\infty$ and $\xi\to\infty$, respectively, in Eq.(41) or (42) and using the corresponding infinity condition (20) or (21) by replacing (x,y) with (ξ,η).

To find R_1, it is noted from Eqs.(20) and (31), respectively, that

$$\phi_1(\xi,\eta) = R_1\phi_0(-\xi,\eta) \qquad \text{as} \quad \xi\to-\infty \tag{43}$$

$$G_1(x,h;\xi,\eta) = -\frac{2\pi \mathrm{i}K\sinh kh'\cosh k(h-\eta)}{(1-\rho)\Delta'(k)\mu\sinh kh}\mathrm{e}^{\mathrm{i}\mu(x-\xi)} \quad \text{as} \quad \xi\to-\infty \tag{44}$$

Substituting Eq.(43) and (44) into Eq.(41) R_1 is obtained as

$$R_1 = -\frac{\mathrm{i}K\sinh kh'}{(1-\rho)\mu\Delta'(k)}\int_{-\infty}^{\infty}\mathrm{e}^{\mathrm{i}\mu x}p(x)\mathrm{d}x= -\frac{\mathrm{i}Kk\sinh kh'\cos 2\theta\sec\theta}{(1-\rho)\Delta'(k)\sinh kh}\int_{-\infty}^{\infty}\mathrm{e}^{2\mathrm{i}k(\cos\theta)x}c(x)\mathrm{d}x \tag{45}$$

(using $\mu = k\cos\theta$)

Similarly, to find T_1, it is also noted from Eq.(20) and (31), respectively, that

$$\phi_1(\xi,\eta) = T_1\phi_0(\xi,\eta) \quad \text{as} \quad \xi\to\infty \tag{46}$$

$$G_1(x,h;\xi,\eta) = -\frac{2\pi \mathrm{i}K\sinh kh'\cosh k(h-\eta)}{(1-\rho)\Delta'(k)\mu\ \sinh kh}\mathrm{e}^{-\mathrm{i}\mu(x-\xi)} \quad \text{as} \quad \xi\to\infty \tag{47}$$

Substituting Eqs.(46) and (47) in Eq.(41) T_1 is obtained as

$$T_1 = \frac{\mathrm{i}Kk\sinh kh'\sec\theta}{(1-\rho)\Delta'(k)\sinh kh}\int_{-\infty}^{\infty}c(x)\mathrm{d}x \tag{48}$$

It is also verified that the same expressions for R_1 and T_1 are obtained by letting $\xi\to-\infty$ and $\xi\to\infty$, respectively, in Eqs.(21) and (35), and solving Eq.(42). So the first order reflection and transmission coefficients can be evaluated from Eqs.(45) and (48), respectively, once the shape function $c(x)$ is known. Here, if $\theta=0$ is taken (i.e., the case of normal incidence), then the above results (45) and (48) coincide with the corresponding results as seen in Mohapatra and Bora (2009b).

Now the effects of reflection and transmission are examined for some special forms of the shape function $c(x)$.

5 Special forms of the bottom surfaces

Here, different special forms of shape function $c(x)$ are considered for the uneven bottom surface. As mentioned earlier, these functional forms of the bottom disturbance closely resemble some naturally occurring obstacles formed at the bottom due to sedimentation and ripple growth of sands. Because of the importance of the bed topographies with sinusoidal ripples from the application point of view, emphasis is laid upon them.

5.1 Sinusoidal ripple (Example-1)

A special form of the shape function $c(x)$ is considered in the form of a patch of sinusoidal bottom ripples on an otherwise flat bottom:

$$c(x) = \begin{cases} a\sin(lx+\delta'), & L_1\le x\le L_2 \\ 0 & \text{otherwise}\end{cases} \tag{49}$$

For continuity of the bed elevation one can take

$$L_1 = \frac{-n\pi-\delta'}{l},\quad L_2 = \frac{m\pi-\delta'}{l}$$

where m and n are positive integers and δ' is a constant phase angle. This patch of sinusoidal ripples on the bottom surface with amplitude a consists of $(n+m)/2$ ripples having the same wave number l. For this case, the reflection and transmission coefficients R_1 and T_1, respectively, are obtained as

$$R_1 = -\frac{\mathrm{i}aKk\sinh kh'\cos 2\theta\sec\theta}{(1-\rho)\Delta'(k)\sinh kh}\times \frac{l}{l^2-(2\mu)^2}\left[(-1)^n\mathrm{e}^{2\mathrm{i}\mu L_1}-(-1)^m\mathrm{e}^{2\mathrm{i}\mu L_2}\right] \tag{50}$$

$$T_1 = \frac{\mathrm{i}aKk\sinh kh'\sec\theta}{(1-\rho)\Delta'(k)\sinh kh}\left[\frac{(-1)^n-(-1)^m}{l}\right] \tag{51}$$

For the specific case when there is an integer number of ripples wavelengths in the patch $L_1\le x\le L_2$ such that $m=n$ and $\delta'=0$, the reflection and transmission coefficients are found, respectively, as

$$R_1 = -\frac{aK\sinh kh'\cos 2\theta\sec\theta}{(1-\rho)\Delta'(k)\sinh kh}\frac{(-1)^m(2k/l)}{1-(\beta)^2}\sin(m\pi\beta) \tag{52}$$

$$T_1 = 0 \tag{53}$$

where $\beta = 2\mu/l$.

Eq.(52) illustrates that for a given number of m ripples, the first order reflection coefficient R_1 is an oscillatory function of β which is the ratio of twice the x-component of the interface wave number to the ripple wave number. Furthermore, when the bed wave number is approximately twice the component of the interface wave number along the x-axis, that is, $2\mu/l \approx 1$, the theory predicts a resonant interaction between the bed and the interface. Hence, it is found from Eq.(52) that near resonance the limiting value of the reflection coefficient assumes the value

$$R_1 = \frac{aK\sinh kh'\cos 2\theta\sec^2\theta}{2(1-\rho)\Delta'(k)\sinh kh} m\pi \tag{54}$$

Note that when $2\mu/l$ approaches 1 and m becomes large, the reflection coefficient becomes unbounded contrary to the assumption that R_1 is a small quantity, being the first-order correction of the infinitesimal reflection. Consequently, only the cases excluding these two conditions are considered in order to avoid the contradiction arising out of resonant cases.

Thus, the reflection coefficient R_1, in this case, becomes a constant multiple of m, the number of ripples in the patch. Hence, the reflection coefficient R_1 increases linearly with m. Although the theory breaks down when $\beta = 1$, that is, $2\mu = l$, a large amount of reflection of the incident wave energy by this special form of bed surface will be generated in the neighborhood of the singularity at $\beta = 1$.

As this is a non-dissipative system and since $T_1 = 0$ and R_1 may be large, it is likely to witness a violation in the conservation of energy in the solution for the potentials. Actually the solution is required to satisfy a condition with respect to wave energy flux, i.e., the incident component of wave energy flux on the undulating part is to be balanced approximately by the sum of the reflected and transmitted components. This requirement may not be fulfilled by the expressions for the reflection and transmission coefficients derived here. The reason for the imbalance is that the linearized analysis does not permit any attenuation of the incident interface waves as it travels over the region $L_1 \le x \le L_2$, which causes the predicted reflected wave in the perturbation solution to be overestimated and the transmitted wave to be very small or zero. In practice, if the reflection wave is non-zero, there must be a progressive attenuation of the incident interface waves over the region $L_1 \le x \le L_2$. Davies (1982) has suggested a corrective procedure to establish a proper energy balance in the solution.

5.2 Sinusoidal ripple with two wave numbers (Example-2)

Now, another special form is considered for the shape function $c(x)$ in the form of a patch of sinusoidal ripples on the bottom surface

$$c(x) = \begin{cases} a_1\sin(l_1 x), & L_3 \le x \le 0 \\ a_1\sin(l_2 x), & 0 \le x \le L_4 \\ 0, & \text{otherwise} \end{cases} \tag{55}$$

Here also, for continuity of the bed elevation,

$$L_3 = \frac{-n\pi}{l_1},\ L_4 = \frac{m\pi}{l_2}$$

can be taken where m and n are positive even integers. This is a patch of sinusoidal ripples on the bottom surface with amplitude a_1 on an otherwise flat bottom. The patch in the region $L_3 \le x \le 0$ consists of $n/2$ number of ripples having the wave number l_1 and the patch in the region $0 \le x \le L_4$ consists of $m/2$ number of ripples having the wave number l_2.

Substituting the value of $c(x)$ from Eq.(55) into Eqs.(45) and (48), the reflection coefficient R_1 is obtained along with transmission coefficient T_1, respectively, as follows:

$$R_1 = -\frac{\mathrm{i}a_1 Kk\sinh kh'\cos 2\theta\sec\theta}{(1-\rho)\Delta'(k)\sinh kh}\times \left\{\frac{l_1}{l_1^2-(2\mu)^2}\left[(-1)^n \mathrm{e}^{2\mathrm{i}\mu L_3}-1\right]+\frac{l_2}{l_2^2-(2\mu)^2}\left[1-(-1)^m \mathrm{e}^{2\mathrm{i}\mu L_4}\right]\right\} \tag{56}$$

$$T_1 = \frac{\mathrm{i}a_1 Kk\sinh kh'\sec\theta}{(1-\rho)\Delta'(k)\sinh kh}\left\{\frac{\left[(-1)^n-1\right]}{l_1}+\frac{\left[1-(-1)^m\right]}{l_2}\right\} \tag{57}$$

In this case, if $m = n,\ a_1 = a$ and $l_1 = l_2 = l$, in Eqs.(56) and (57), respectively, then they are reduced to Eqs.(52) and (53) of the previous example, where all the ripples have the same wave number l and amplitude a.

As in Example-1, here also when the bed wave number is approximately twice the component of the interface wave number along the x-axis, that is, $l_1 \approx 2\mu$ and $l_2 \approx 2\mu$, the theory predicts a resonant interaction between the bed and the interface. Hence, under this condition, the limiting value of reflection coefficient R_1 from Eq.(56) is found as

$$R_1 = \frac{a_1 K\sinh kh'\cos 2\theta\sec^2\theta}{4(1-\rho)\Delta'(k)\sinh kh}(m+n)\pi \tag{58}$$

As in Example-1, here also it is observed that R_1 is a constant multiple of $(m+n)/2$, the total number of ripples in the patch of the deformation. Hence, the reflection coefficient R_1 increases linearly with m and n. Although the theory breaks down when either $l_1 = 2\mu$ or $l_2 = 2\mu$, a large amount of reflection of the incident wave energy by this special form of bed surface will be generated in the neighborhood of the singularities at $l_1 = 2\mu$ or $l_2 = 2\mu$.

6 Numerical results and discussions

In this section, the numerical computation and graphical presentation related to the two special forms of bottom surfaces mentioned in the previous section are shown for the first-order reflection and transmission coefficients.

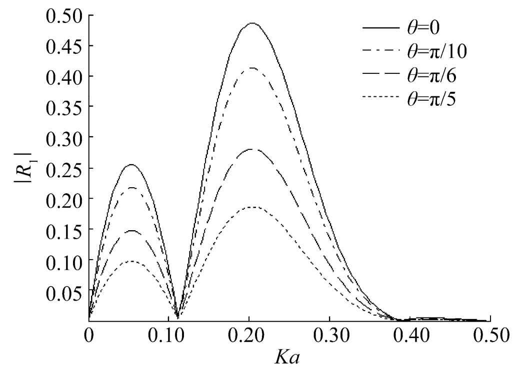

Fig. 2 Reflection coefficient $|R_1|$ plotted against Ka for la=0.52 and m=2

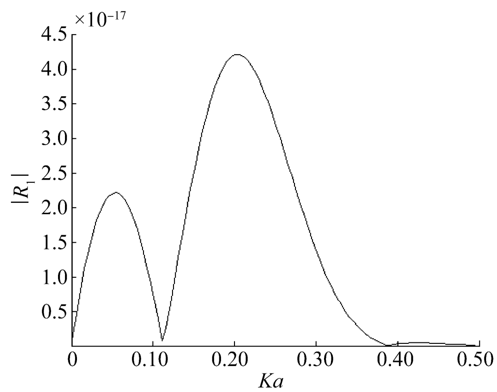

Fig. 3 Reflection coefficient $|R_1|$ plotted against Ka for la=0.52; m=2; $\theta = \pi/4$

In Example-1, a patch of sinusoidal bottom undulations on the channel bed is considered because of its considerable physical significance in the ability of an undulating bed to reflect incident wave energy which is important for a channel flow consisting of a two-layer fluid. The numerical computations are considered for the non-dimensionalized first-order reflection coefficient $|R_1|$, which is calculated from (52), due to an oblique incident wave at an angle θ on the undulating bed of ripple wave number l having m number of ripple wavelengths in the patch. In Fig. 2, different curves of $|R_1|$ are shown against Ka for $\rho = 0.95$, $h = 10a$, $h' = 10a$, $la = 0.52$, $m = 2$, $\theta = 0; \pi/10; \pi/6$; and $\pi/5$. It may be noted that for $\theta = 0$ (the case of normal incidence), the maximum value of $|R_1|$ is 0.485 77, attained at μa =0.212 02 (when $Ka = 0.206$), that is, when the ripple wave number la of the bottom undulation becomes approximately twice as large as the interface wave number μa. The same can be observed when the value of θ is non-zero (the case of oblique incidence). Another common feature in Fig. 2 is the oscillating nature of the absolute values of the first-order coefficients as functions of the wave number Ka. In Fig. 3, $|R_1|$ is plotted against Ka for $la = 0.52$, $m = 2$, and $\theta = \pi/4$. For this value of θ, the reflection coefficient $|R_1|$ is much less (almost negligible) compared to the other angles of oblique incidence, *e.g.*, $\theta = \pi/6$, $\pi/5$. As the angle of incidence θ increases, the peak value of $|R_1|$ decreases. For the case of normal incidence, the peak value of $|R_1|$ is the largest.

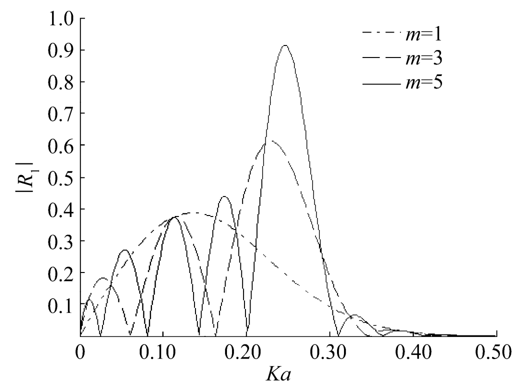

Fig. 4 Reflection coefficient $|R_1|$ plotted against Ka for θ =0 and la=0.52

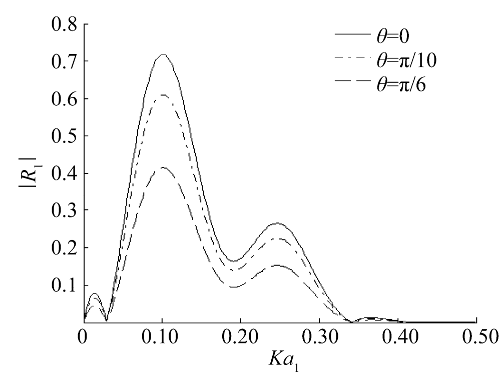

Fig. 5 Reflection coefficient $|R_1|$ plotted against Ka_1 for l_1a_1 =0.52; l_2a_1 =0.26; n=3 and m=2

In Fig. 4, different curves correspond to different numbers of ripples $m = 1,3,5$ in the patch of the undulation. In this figure, for all curves, $\theta = 0$, $\rho = 0.95$, $h = 10a$, $h' = 10a$, $la = 0.52$ are considered. The curve which corresponds to $m = 1$, the maximum value of $|R_1|$, is 0.38698, attained at μa =0.150 19 (when $Ka = 0.136$). Similarly for the curve corresponding to $m = 3$, the maximum value of $|R_1|$ is 0.612 18attained at μa =0.235 22 (when Ka =0.231) and for the curve corresponding to $m = 5$, the maximum value of $|R_1|$, is 0.914 14 attained at μa =0.249 38 (when $Ka = 0.246$). From Fig. 4, it is clear that the peak value of $|R_1|$ is attained when the ripple wave number la of the bottom undulation becomes approximately twice as large as the interface wave number μa. As m, the number of ripples increases, and the value of μa converges to a number in the neighborhood of 0.26, *i.e.*, for $la/2$, where $|R_1|$ attains its maximum, and the peak value of non-dimensionalized reflection coefficient $|R_1|$ also increases. Its oscillatory nature against Ka is more noticeable with the number of zeros of $|R_1|$ increased but the general feature of $|R_1|$ remains the same.

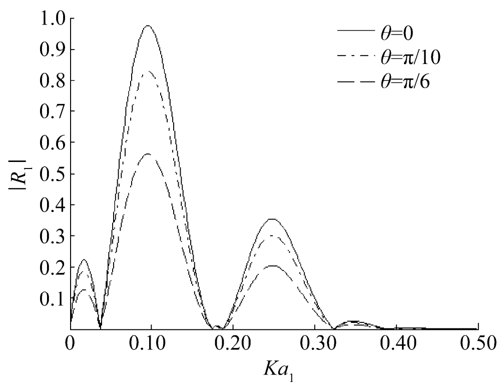

Fig. 6 Reflection coefficient $|R_1|$ plotted against Ka_1 for l_1a_1 =0.52; l_2a_1 =0.26; n=4 and m=2

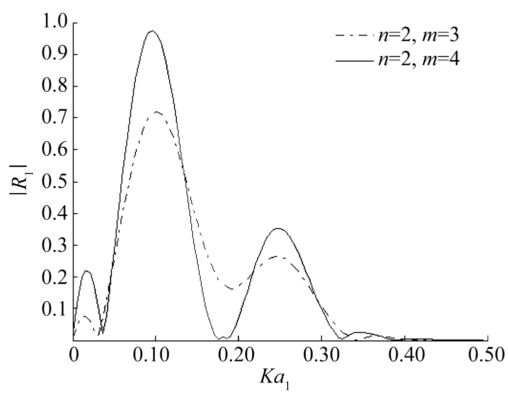

Fig. 7 Reflection coefficient $|R_1|$ plotted against Ka_1 for θ =0; l_1a_1 =0.26 and l_2a_1 =0.52

In Example-2, another special patch of sinusoidal bottom undulations with ripples having two different wave numbers l_1 and l_2 is considered instead of a single ripple wave number of the previous example. For this example, the numerical computations are considered for the non-dimensionalized first-order reflection coefficient $|R_1|$, which is calculated from (56), due to an obliquely incident wave on the undulating bed in the lower layer at an angle θ to the positive x-axis with the undulation having two different ripple wave numbers l_1 and l_2, respectively, and m and n number of ripple wavelengths in the patch. Here $\rho = 0.95$, $h = 10a_1$ and $h' = 10a_1$ are again considered. In Fig. 5, $|R_1|$ is plotted against Ka_1 for $l_1a_1 = 0.52$, $l_2a_1 = 0.26$, $n = 3$, $m = 2$, and $\theta = 0$, $\pi/10$, $\pi/6$. It may be noted that for $\theta = 0$ (the case of normal incidence), the first maximum value of $|R_1|$ is 0.717 58, attained at μa_1 =0.120 8 (when $Ka_1 = 0.101$). The second maximum value of $|R_1|$ that corresponds to the same ($\theta = 0$) curve is 0.264 4, attained at μa_1 =0.249 38 (when $Ka_1 = 0.246$). The same general feature can be observed for other non-zero values of θ (the case of oblique incidence). Again, as the angle of incidence θ increases, the peak value of $|R_1|$ decreases. For the case of normal incidence, the peak value of $|R_1|$ is the largest. In Fig. 6, $|R_1|$ is plotted against Ka_1 for $l_1a_1 = 0.52$, $l_2a_1 = 0.26$, $n = 4$, $m = 2$, and $\theta = 0$, $\pi/10$, $\pi/6$. In this case the number of ripples increases from $n = 3$, $m = 2$ to $n = 4$, $m = 2$. In Fig. 6, for $\theta = 0$, the first maximum value of $|R_1|$ is 0.974 56, attained at μa_1 =0.116 63 (when Ka_1 =0.096) and second maximum value of $|R_1|$ is 0.352 62, attained at μa_1 =0.249 38 (when $Ka_1 = 0.246$). Therefore, it is observed from this figure that for any angle θ, $0 \le \theta < \pi/2$, $|R_1|$ has two peak values which are attained when the ripple wave numbers l_1a_1 and l_2a_1 of the bottom undulation become approximately twice as large as oblique interface wave number μa_1, and if the angle of incidence increases, the value of $|R_1|$ decreases. Again, as the numbers of ripples, n and m, increase, the peak value of non-dimensionalized reflection coefficient $|R_1|$ increases, and its oscillatory nature against Ka_1 is more noticeable with the number of zeros of $|R_1|$ increased, but the general feature of $|R_1|$ remains the same.

In Fig. 7, $|R_1|$ is plotted against Ka_1 for $\theta = 0$, $l_1a_1 = 0.26$, $l_2a_1 = 0.52$, $n = 2$, and m =3. In the second curve, the number of ripples increases from $n = 2$, m =3 to $n = 2$, m =4. From the figure it is observed that even if the roles of l_1a_1 and l_2a_1 are reversed, the same conclusion can be drawn as was previously with Figs. 5 and 6.

7 Conclusions

The work described in this paper is an extended work of the problem of water wave scattering by a bottom deformation in a two-layer fluid, when a rigid horizontal lid, which forms the horizontal upper boundary of a channel, replaces the free surface. In such a situation propagating waves can exist at only one wave number for any given frequency. By developing a suitable perturbation technique, the problem is reduced to a coupled boundary value problem to the first-order of the potentials and the coefficients which is solved by a method based on Green's integral theorem with the introduction of appropriate Green's functions. First order approximations to the reflection and transmission coefficients are obtained in terms of computable integrals and depicted graphically by a number of plots. The main advantage of this method, demonstrated through the example of a patch of sinusoidal ripples, is that a very few ripples may be needed to produce a substantial amount of reflected energy. It is also observed that for small angles of incidence, the reflected energy is more as compared to other angles of incidence up to $\pi/4$. Another main result that follows is that for the ripples having two different wave numbers, the resonant interaction between the bed and the interface attains in the neighborhood of the singularity when the ripple wave numbers of the bottom undulation become twice the interface wave number. The problem and solution method described here differ from the previous works on the subject in the sense that the free surface has been approximated by a horizontal wall and the bottom surface contains deformation. The solution developed here is expected to be helpful in considering two-layer fluid problems in a channel with an uneven bottom.

Acknowledgement

The first author wishes to thank Council of Scientific and Industrial Research (CSIR), Government of India, for providing senior research fellowship for pursuing PhD at Indian Institute of Technology Guwahati, India (2007–2009), where this work was initiated.

References

Bhatta DD, Debnath L (2006). Two layer transient water waves over a viscoelastic ocean bed. *Journal of Applied Mathematics and Computing*, **22**, 133-147.

Chamberlain PG, Porter D (2005). Wave scattering in a two-layer fluid of varying depth. *Journal of Fluid Mechanics*, **524**, 207-228.

Davies AG (1982). The reflection of wave energy by undulations of the sea bed. *Dynamics of Atmosphere and Oceans*, **6**, 207-232.

Kassem SE (1986). Wave source potentials for two superposed fluids, each of finite depth. *Mathematical Proceedings of Cambridge Philosophical Society*, **100**, 595-599.

Lamb H (1932). *Hydrodynamics*. 6th ed, Cambridge University Press, Cambridge, UK.

Linton CM, Cadby JR (2002). Scattering of oblique waves in a two-layer fluid. *Journal of Fluid Mechanics*, **461**, 343-364.

Linton CM, McIver M (1995). The interaction of waves with horizontal cylinders in two-layer fluids. *Journal of Fluid Mechanics*, **304**, 213-229.

Maity P, Mandal BN (2006). Scattering of oblique waves by bottom undulations in a two-layer fluid. *Journal of Applied Mathematics and Computing*, **22**, 21-39.

Mandal BN, Basu U (1993). Diffraction of interface waves by a bottom deformation. *Archives of Mechanics*, **45**(3), 271-277.

Mandal BN, Basu U (1996). Oblique interface-wave diffraction by a small bottom deformation in two superposed fluids. *Archives of Mechanics*, **19**(2)**,** 363-370.

Mei CC (1985). Resonant reflection of surface water waves by periodic sandbars. *Journal Fluid Mechanics*, **152**, 315-335.

Miles JW (1981). Oblique surface wave diffraction by a cylindrical obstacle. *Journal of Atmosphere and Oceans*, **6**, 121-123.

Mohapatra S, Bora SN (2009a). Water wave interaction with a sphere in a two-layer fluid flowing through a channel of finite depth. *Archive of Applied Mechanics*, **79**, 725-740.

Mohapatra S, Bora SN (2009b). Scattering of internal waves in a two-layer fluid flowing through a channel with small undulations. *Ocean Dynamics*, **59**, 615-625.

Mohapatra S, Bora SN (2011). Reflection and transmission of water waves in a two-layer fluid flowing through a channel with undulating bed. *Zeitschrift fur Angewandte Mathematik und Mechanik*, **91**(1), 46-56.

Sturova IV (1994). Planar problem of hydrodynamic shaking of a submerged body in the presence of motion in a two-layered fluid. *Journal Applied Mechanics and Technical Physics*, **35**, 670-679.

Sturova IV (1999). Problems of radiation and diffraction for a circular cylinder in a stratified fluid. *Fluid Dynamics*, **34**, 521-533.

Smrutiranjan Mohapatra received his M.Sc. from Sambalpur University, India, and his PhD from the Indian Institute of Technology, Guwahati, India in 2009. He also worked as a post doctoral fellow at the Indian Institute of Science, Bangalore, India, prior to accepting his present position of Assistant Professor in the Department of Mathematics, Institute of Chemical Technology Mumbai, India. His main areas of interest are water wave scattering and two-layer fluid. He has approximately 10 research publications to his credit.
e-mail: sr.mohapatra@ictmumbai.edu.in

Swaroop Nandan Bora received his M.Sc. from the University of Delhi, India, and his PhD from Dalhousie University, Halifax, Canada, in Engineering Mathematics. He is an Associate Professor in the Department of Mathematics, Indian Institute of Technology, Guwahati, India. His research interests focus on water waves, flows through porous media, and special functions. He has 23 research publications to his credit and is involved in a number of sponsored projects.
e-mail: swaroop@iitg.ernet.in